# DETAILED INVESTIGATION OF A VAPORISING FUEL SPRAY

## PART I: EXPERIMENTAL INVESTIGATION OF TIME AVERAGED SPRAY

by

A. J. Yule, C. Ah Seng, R. Boulderstone, A. Ungut,

P. G. Felton and N. A. Chigier

Combustion Aerodynamics Research Laboratory
Department of Chemical Engineering and Fuel Technology
University of Sheffield, England

July 1980



Progress Report for Contract with
NASA-Lewis Research Center

CARL Report No.
CARL IM 80-3

## CONTENTS

## SUMMARY

Measurement techniques, with good spatial resolution, have been used to investigate the structures of turbulent kerosene fuel sprays under cold conditions and under conditions of vaporisation in hot surrounding air-streams. A novel laser tomographic light scattering technique has been used for the detailed mapping of internal spray structure. This technique is demonstrated to provide rapid and accurate, high resolution measurements of droplet sizes, concentrations and vaporisation. Measurements using a computer interfaced thermocouple are presented and it is found that the potential exists for separating gas and liquid temperature measurements and diagnosing local spray density by in situ analysis of the response characteristics of the thermocouple. The thermocouple technique is shown to provide a convenient means for measuring mean gas velocity in both hot and cold two-phase flows.

The experimental spray is axisymmetric and has carefully controlled initial and boundary conditions. The flow is designed to give relatively insignificant transfer of momentum and mass from spray to air flow. The data obtained in this test spray give fundamental insight into the various processes occurring in turbulent spray vaporisation and provide a data base for modelling work. In particular the effects of (i) size-dependent droplet dispersion by the turbulence, (ii) the initial spatial segregation of droplet sizes during atomisation and (iii) the interaction between droplets and coherent large eddies are diagnosed.

## 1. INTRODUCTION

Past investigations which concerned the vaporisation or burning of liquid fuel sprays can generally be divided into either fundamental investigations, involving single or simple one-dimensional arrays of monosize droplets, or investigations of complex 'practical' combustion systems. It is considered that the former case has been proved to be oversimplified; for example, the 'cloud' effects of many droplets have been shown to be of extreme importance in determining the environment and thus the vaporisation, ballistics and burning of droplets. On the other hand investigations of the latter case, whilst revealing important information on overall spray structures[1, 2, 3] have not significantly improved our modelling approaches to fuel sprays because the flows studied did not, for example, permit a straightforward specification of initial and boundary conditions. It is thus considered to be of both practical and fundamental interest to make very detailed investigations of the structures of sprays which are neither oversimplified nor so complex that data interpretation becomes impossible.

In this way one might hope to provide data to enable the improvement of modelling approches to spray structure under conditions of practical interest but without the complexities introduced by ill-defined initial conditions, non-axisymmetry, recirculation etc. Both experimental[1] and analytical[4] results show that in most practical situations spray burning, rather than being controlled by 'single droplet burning' is a 'droplet cloud' process, in which the majority of droplets vaporise in groups and reaction occurs at the vapour/air interface surrounding the clouds; similar to a gas diffusion flame. Thus modelling of spray burning requires modelling of droplet vaporisation and droplet-turbulence interaction under conditions of heat, momentum and mass transfer, between the droplets and the surrounding gas, which do not generally involve regions of reaction close to the droplet surface. Furthermore the 'cloud vaporisation' process, which occurs generally for most of the liquid fuel injected into the spray, ensures that the environment (and thus the vaporisation and ballistics) of each individual droplet is controlled by the vaporisation and ballistics of many surrounding droplets.

Vaporisation of liquid sprays is also an important process in its own right, even when the spray is not burning. In particular the premixed-prevaporised gas turbine combustor process requires fuel sprays to be completely vaporised and mixed with air before reaction occurs in the combustion chamber. In order that prediction methods can be used to design such systems, basic fundamental data is required on droplet vaporisation and ballistics in heated gas streams.

In the basic experiment described below a twin fluid atomiser kerosene spray injected into a coflowing secondary stream which can be preheated, is investigated. The spray is designed to be axisymmetric and the secondary flow is uniform and with low turbulence intensity. The throughputs of atomising air and fuel, and the atomiser geometry, were selected to simplify the spray

sufficiently so that certain of the processes which can occur in spray-turbulence interaction were minimised. For example, although the phenomena of droplet/gas velocity lag occurred near the atomiser, so that droplets accelerate to the gas velocity in the initial part of the spray, the total momentum of the liquid phase, at any station is always very much less than the momentum of the gas phase, i.e. in the jet produced by the atomising air. In the same way the total fuel vapour mass flow rate, at any axial station, is always very much less than the local air mass flow rate contained in the jet. These conditions result in the simplifying approximation that the gas flow field, in the spray studied, is the same as that in the jet produced by the atomising air alone. Furthermore fine sprays are utilised so that the further simplifying assumption can be made that most of the droplets, eventually, closely follow the local turbulent gas flow field at some distance downstream.

These experiments are the initial stage of an investigation which has the objectives:

(i) to provide fundamental insight and data on droplet vaporisation-turbulence interaction;

(ii) to provide a data base for model development and evaluation;

(iii) to develop and utilise new diagnostic techniques for the investigation of internal spray structure.

An important feature, stressed in this report, is the demonstration of a new 'laser-tomographic' light scattering technique for investigating spray structure. This technique is shown to provide a means for the rapid and accurate mapping of droplet size distributions and volume concentrations in sprays. The technique provides a means of measuring vaporisation rates rapidly, without probe intrusion, and without the data analysis problems associated with imaging techniques such as holography and photography.

## 2. APPARATUS

Figure 1 shows the apparatus for the central injection of the kerosene spray into a coflowing secondary air stream. The secondary air could be preheated by banks of electrical heaters. Smoothing screens gave turbulence levels of approximately 1% in the secondary flow, which had a uniform velocity across 90% of the secondary nozzle diameter.

Figure 2 shows the design of the twin fluid atomiser which was constructed from hypodermic tubing. The atomising air and kerosene flow rates were measured by calibrated rotameters. Table 1 shows the various parameters for the test spray.

The complete nozzle assembly, shown in Figure 1, could be traversed both vertically and radially. The spray and gas stream

were collected by an extraction system 0.3 m below the atomiser. Tests showed that the extract system had no effect on the flow in the first 0.14 m length of spray. The various probes, described below, were fixed in position and the spray was moved to provide a complete mapping of the flow.

## 3. MEASUREMENT TECHNIQUES

### Laser Tomography

Particle size distributions were determined using a Malvern Instruments ST1800 Particle Size Meter. A parallel He/Ne laser beam is passed through the spray and the forward scattered light is collected by a Fourier transform lens. The radial light power distribution is measured using a photodetector consisting of 30 concentric annulli placed in the focal plane of the lens, and the particle size distribution is calculated from this using Fraunhofer diffraction theory.[5, 6] Total particle concentration was determined by measuring the total forward scattered light power - this is not an absolute measurement as all the optical constants are not known and must be calibrated.

This instrument rapidly gives an 'overall' size distribution for a complete width of the spray. The line-integral nature of the particle size distribution does not give any information on the drop size distribution across the spray. However, if a number of line integral measurements are made through different parts of the spray, the scattered light data can be transformed into two-dimensional distributions of drop size distribution and concentration in a plane through the spray. This data transformation is termed 'tomography' and has been applied to several systems in recent years, particularly for medical X-ray brain and body scanners. For the case of an axisymmetric system such as the spray being studied the transformation is greatly simplified, only one set of parallel scans through the spray being required (this is analagous to the Abel transformation used in flame spectroscopy studies). Full details of the procedure are given in a recent paper.[7]

The apparatus was set up as shown in Figure 3, the 2 mm diameter laser beam being shone through the spray and the forward scattered light collected by the Fourier Transform lens and the signal from the detector transmitted to a PDP8A minicomputer. The beam is held in a fixed position and the spray moved relative to the beam.

The transformation procedure was verified using a Spraying Systems type II atomiser which produces an axisymmetric full cone spray. A 9 mm diameter laser beam was used and spark photographs were also taken at intervals of 9 mm across the spray along the camera axis. Sufficient photographs were taken at each point to permit measurement of at least 2,000 in focus droplets. The photographs were analysed by a Cambridge Instruments Image Analysis Computer using a technique developed by Yule.[8] The

volume median diameters, $d_{v0.5}$, and relative spans, $(d_{v0.8} - d_{v0.2})/d_{v0.5}$, obtained using both techniques, are plotted against radial distance across the spray in Figure 4. The local spatially averaged volume concentrations of liquid droplets are plotted against radial distance in Figure 5, the values are normalized by the peak value where the measured volume concentration is $8.7 \times 10^{-2}$% by volume. Excellent agreement was obtained for all parameters, thus confirming the validity of the procedure.

Thermocouples

A computerised thermocouple technique, first described by Yule et al.,[9] has been used. The thermocouples consisted of 10 mm lengths of 25 μm diameter 'chromel' and 'alumel' wires which were flame welded together and mounted between 0.5 mm diameter Chromel-Alumel support wires. The output is fed via a low noise battery dirven preamplified to an ADC and fed as 12 bit words to a PDP-11 computer. For the purpose of thermocouple response characteristics measurement,[9] a square wave overheating voltage was applied to the thermocouple, with characteristics governed by the PDP-11 program. The thermocouple e.m.f. decay after each overheating pulse is digitised and acquired by the computer. By ensemble averaging the decay curves, variations caused by temperature fluctuations in the flow are averaged out. The resulting decay curve permits determination of the insitu thermocouple response characteristics, usually in the form of the first order characteristics determined by a time constant $\tau$ where

$$T_g = T_m + \tau\delta(T_g - T_m)/\delta t$$

and $T_g$ and $T_m$ are the instantaneous gas temperature and measured temperature respectively. In these experiments measurements of $\overline{T}_g$ and $\tau$ are made in various flows. The determination of mean gas velocity from measurements of $\tau$ is investigated. For the case of thermocouple measurements inside the sprays particular care should be taken because of the potential 'influences' of impacting droplets on the wire. These effects are considered in Section 5 where consideration is also given to the potential application of the liquid cooling effect to enable the derivation of local spray density by using the computerised thermocouple.

Laser Anemometer

Velocity measurements were carried out using an OEI laser anemometer system with a 1W Lexel 85.1 Argon ion laser operating on the green line. An off-axis forward scattering arrangement was used with a fringe spacing and measurement volume dimensions 3.2 micron and 1mm x 0.1mm x 0.1mm. Signals were processed by a Cambridge Consultants tracker. Gas flow measurements were made by seeding the secondary flow with 1 μm droplets by using an OEI particle generator.

## 4. EXPERIMENTAL RESULTS

Measurements have been made for four flow conditions:

Case (i): 'Cold' secondary air (293K), cold atomising air, no kerosene.

Case (ii): Cold secondary air, cold atomising air, with kerosene.

Case (iii): 'Hot' secondary air (450K), cold atomising air, no kerosene.

Case (iv): Hot secondary air, cold atomising air, with kerosene.

The sprays for both the cold and hot cases (cases (ii) and (iv)) had the same initial conditions as specified in Table 1. The mass flow rate of the secondary air was maintained the same for the hot and cold flow cases.

### Tomographic Light Scattering Measurements

Figure 6 shows distributions of spatially averaged volume concentrations of liquid droplets measured by the light scattering technique in what will be referred to as the 'cold' and 'hot' sprays (cases (ii) and (iv) above). The figures show the rapid reduction in liquid phase volume concentration in the hot spray compared with the cold spray. The distributions are approximately Gaussian in shape for both the hot and cold cases. For the cold spray the peak concentration varies approximately as $x^{-1}$ and the concentration 'half-width' increases, initially, approximately linearly with x. The proportionalities are to be expected for a passive scalar distribution in a self-preserving gas jet. Although the droplet concentration cannot be considered as a passive scalar in the true sense, this is evidence that most of the droplets are small enough to follow the flow field of the air jet produced by the atomising air. With increasing distance downstream there is a decrease in the rate of spread of the concentration distribution. This is likely to be attributable to the confining effect of the secondary stream. Beyond x = 80 mm, for the hot spray case, the scatter in the concentration measurements increases significantly, due to the relatively low scattered light power from the low droplet concentrations. In future experiments the signal to noise ratio will be improved by increasing the laser power. Near the nozzle, particularly at x = 20 mm, there are very high droplet concentration gradients so that the spatial resolution defined by the 2 mm beam diameter will introduce some measurement error. Future developments of this technique for small scale sprays such as this will utilise beams with smaller diameters.

The measurements of mass mean droplet diameters are presented in Figure 7 for both the 'hot' and 'cold' sprays. These are tomographically transformed data dnd they thus represent 'point' measurements of mean droplet size. It is seen that, for

both the hot and cold cases, there is a region of larger droplets at the outer region of the spray. Comparison with the volume concentration data (Fig. 6) shows that these outer regions of larger droplets contain only a small proportion of the total droplet volume. The droplet volume and concentration data are spatially averaged. In terms of liquid volume flux, the larger droplets also contribute little to the total flow rate, due to the lower velocities of the outer part of the spray. For the cold spray case there is little change in mean drop size with increasing distance downstream. However for the hot spray case there is a gradual increase in mean drop size which can be attributed to the preferential vaporisation of the smaller droplets. The data are discussed further, in the light of the other measurements, in Section 5 below.

Figure 8 shows measurements of the relative span of the size distribution for the hot and cold sprays. The relative span is a measure of the width of the size distribution and it is here defined by the ratio $(d_{v0.8} - d_{v0.2})/d_{v0.5}$ where the z fraction of the spray by volume consists of droplets having diameters smaller than $d_{vz}$. The major trend in Figure 8 is the relative narrowing of size distributions in the hot spray with increasing distance downstream. This can again be attributed to the preferential vaporisation of the smaller droplets. For the cold case vaporisation is expected to be small and photographs showed that atomisation had been completed by x = 20 mm. Thus the changes noted in the relative span distributions in the cold spray must be attributable largely to the dispersion of droplets in the turbulent flow. In particular the initial radial segregation of droplet sizes near the atomiser is dispersed. The dispersion rates vary according to droplet size.

Laser Anemometer Measurements

Figure 9 shows the mean velocity distribution in case (i), i.e. the cold jet flow without kerosene injection. As will be described, this is also representative of the gas flow field for case (ii), with kerosene. There is seen to be a linear region of jet spread with a virtual origin 20 mm upstream of the atomiser outlet. It is seen that there is negligible interference between the jet (and thus the spray) and the outer mixing layer of the secondary flow for the first 100 mm of flow. Curves representing the spread of the half width of the droplet volume concentration distribution (cold spray) and the half width of the gas velocity distribution, are included in Figure 9. It can be seen that these half widths do not generally coincide and there are differences in the spreading of the droplet and gas velocity fields. This is again indicative of the differing dispersion rates according to the droplet sizes.

Figure 10 compares mean gas velocity and mean droplet velocities at different axial positions in the cold flow. The mean droplet velocity was obtained by analysing the Doppler signals from droplets, without seeding the flow. This velocity is approximately an ensemble averaged velocity for droplets greater than 5 μm. In the second stage of this detailed investigation

of the spray structure, a refined version of the LDA particle sizing technique of Yule et al.[10] will be used to obtain size-velocity information. It can be seen from Figure 10 that beyond x = 80 mm the mean droplet and gas velocities are nearly the same for most of the width of the spray except at the outer edge. It is known that this outer region consists of a dilute region of relatively monodisperse large droplets. These droplets are least likely to move with the local gas velocity, which correlates qualitatively with the LDA results. Care should be taken in interpreting the droplet velocity measurements in the central dense spray near the atomiser because of poor signal/noise ratios. It is considered that measurements using a tracker in this region are biased towards the relatively slow moving larger droplets, which produce relatively high amplitude signals with relatively good signal/noise ratios.

Figures 11 and 12 show comparisons of mean gas and mean droplet velocities for the cold and hot sprays at x = 40 mm and x = 100 mm. It is seen that the heated secondary flow has a velocity increased to 7 m/s, compared to 5 m/s for the cold flow case. This is explained by the expansion effect of heating. The gas and droplet velocities within the spray are also higher for the hot spray than for the cold spray case. This can also be explained by the accelerating effect of the entrainment and mixing of hot air into the spray. As will be described, there are no significant contributions to the higher velocities found within the hot spray, from the release of fuel vapour nor from momentum transfer between the liquid and gas phases (for the particular spray studied here).

Thermocouple Measurements

Figure 13 shows mean temperature distributions in the hot flow, with and without the injection of kerosene. A comparison of radial distributions of temperature measured with and without the atomising air showed that the major contribution to the temperature deficit, for the case without kerosene, came from the boundary layer on the outer surface of the atomiser. Figure 13 shows that there is a significant decrease in the measured mean temperature for the spray case. The extent to which the measured temperature is representative of the gas temperature and the potential cooling effects of droplet impaction on the thermocouple are discussed in Section 5.

Figure 14 shows measurements of the thermocouple time constant in the hot flow, with and without the spray. It is seen that there is little difference between these measurements except in the first positions, near the atomiser, where the spray is dense. This shows that the droplets impacting on the thermocouple affect the transfer characteristics of the probe at high spray densities: however the effect of the droplets in the time constant appears to be less significant than their effect on the measurement of gas temperature.

Figure 15 shows a comparison of the mean velocity measured by laser anemometer for case (i) (i.e. the cold flow without kerosene

injection) and mean velocities derived from the thermocouple time constant measurements by using the heat transfer relationships for a cylinder.[9] The agreement is seen to be excellent. Figure 16 shows a comparison of thermocouple velocity measurements obtained by this technique for cases (iii) and (iv) (i.e. the hot flow without and with kerosene injection). It will be argued that the gas velocity field should not be greatly affected by the injection of kerosene for the particular spray used here. Figure 16 shows that the thermocouple measurements of velocity are very similar for the cases with and without the presence of droplets except for x = 40 mm. This is a clear indication that, below some limiting particle concentration, the relatively simple computerised thermocouple time constant measurement technique can give an accurate measurement of gas velocity in two phase flow under conditions of high temperature and particle impaction. These conditions preclude other probing techniques, and sophisticated techniques are required for separating the signals from large and small particles when using laser anemometry.

## 5. DISCUSSION

The laser tomography technique has been shown to be a valuable measurement technique for rapidly characterising fuel sprays. In Figure 17 the tomographically derived droplet concentration data are presented in the forms of iso-concentration contours of liquid phase, by volume. This gives a clear demonstration of the effect of the heated secondary flow on the spray vaporisation. It is seen that the initial vaporisation, for the hot case, proceeds very rapidly but, beyond approximately x = 60 mm, the vaporisation rate decreases greatly. Comparison with the drop size distribution data in Figures 7 and 8 shows that this downstream region corresponds to a residue of relatively large droplets. In order that the predictions of spray modelling can be compared with these results it was considered to be necessary to measure the spray initial conditions as close to the atomiser as possible. High magnification spark photography has been used. The results will be included in a later report on the second part of this investigation in which a more detailed analysis of the data is made. The time dependent spray structure will be investigated and comparisons with modelling predictions will be made. However from the point of view of the mainly qualitative interpretation of the measurements in terms of spray structure, which is presented here, it is worthwhile describing some aspects of the photographs of the spray near the atomiser. A typical photograph is shown in Figure 18. Atomisation commences as a wave instability of the liquid column leaving the central atomiser orifice. These waves break into 'lumps' of liquid of various sizes and shapes which are then atomised into small droplets. Atomisation is generally completed by x = 10 mm for the particular spray studied. Occasional large lumps of liquid move unusually far radially from the central region of the flow. For these sections of fluid atomisation is not as efficient as for the main bulk of liquid in the central zone. This is presumably because of movement of the liquid into a relatively low

velocity environment with low atomisation potential. This process, observed within a few mm of the atomiser, resulted in the formation of a dilute region of fairly monosize large droplets at the outer region of the spray whilst the central region is polydisperse, with many droplets smaller than 5 μm. As can be seen from Figures 7 and 8 this spatial segregation of droplet sizes which originates during the atomisation process persists for the full length of the spray investigated.

The momenta contained within the gaseous and liquid phases of the sprays have been calculated by, for the gas phase, evaluating the 'excess momentum' of the gas jet $M_g$ (in fact $M_g$ is the rate of transfer of momentum, but the term momentum alone is conventionally used in the context of jet flows)

$$M_g = 2\pi \rho_{gas} \int_0^{\text{EDGE OF JET}} (U_{gas} - U_s)\, U_s\, r\, dr$$

where $U_g$ is the mean gas velocity and $U_s$ is the secondary stream velocity. For a jet in a uniform secondary flow this quantity should be constant. Figure 19 shows $M_g$ values calculated for different values of x in the cold flow. The degree of scatter is reasonable and the results indicate that the assumption that the spray is in a uniform secondary stream is a reasonable approximation up to x = 100 mm. The total momentum (rate) in the spray contained within the liquid phase was also estimated at different x values by integrating the data. The droplet momentum $M_d$ was estimated by the integral

$$M_d(x) = 2\pi \rho_{liquid} \int_0^{\text{EDGE OF SPRAY}} U_{drop}^2\, c\, r\, dr$$

where c is the local liquid phase volume concentration and $U_{drop}$ is the ensemble averaged local droplet velocity. This is an approximation, as account is not taken of correlations between droplet diameters and velocities and, as described above, the measured mean droplet velocity can be biased towards different size ranges, depending upon the local LDA signal quality. Calculated values are included in Figure 19 and it is seen that the liquid phase momentum is always at least one order of magnitude less than that contained within the gas phase. Thus one can expect there to be little effect of the droplets upon the gas velocity field for this particular spray so that the gas flow field without droplets can be measured to give a reasonably accurate description of the flow field in the presence of droplets.

Estimates of the total liquid phase volume flux were also made by integrating the volume concentration and velocity data.

Downstream or 60 mm the calculated values for the cold spray were within 15% of the total kerosene volume flow rate supplied to the atomiser ($9 \times 10^{-2}$ ml/s). This indicates both negligible vaporisation in the cold spray and the accuracy of the light scattering technique. At x = 80 mm in the hot spray, the total liquid phase volume flux had fallen to ($4 \times 10^{-2}$ ml/s) indicating vaporisation of 56% of the droplets by volume.

As shown in Table 1, the initial liquid/air mass ratio is 38%. However the mass ratio of the total vapour phase kerosene/total air flow, at any section of the hot spray, never exceeds 5%. Thus there should also be only a small change in the total spray gas flow characteristics due to the release of kerosene vapour. Straightforward heat balance calculations permitted estimation of the cooling effect, on the gas flow, caused by heat transfer to the droplets to (a) heat droplets to the wet bulb temperature, and (b) provide the latent heat of vaporisation. It is found that, for the hot spray, the cooling effect of droplet vaporisation should result in centre line mean gas temperature reduction of no more than 8° C at x = 40 mm, and 2° C at x = 100 mm. This corresponds to the measured centre line mean temperature reductions of 32° C at x = 40 mm and 17° C at x = 100 mm (see Fig. 13). It is thus clear that, for the spray, the mean temperature measured by the thermocouple is significantly influenced by the impaction of droplets on the thermocouple wire. However, as can be seen in Figure 14, the presence of droplets has noticeably less influence on the time constant of the thermocouple, measured by the square-wave electrical overheating method. Thus the thermocouple time constant can provide a means of measuring gas velocity for droplet volume concentrations (volume of droplets/volume of gas), at least as high as $5 \times 10^{-5}$, which corresponds to a local air/liquid fuel mass ratio of 30. It was found that the shape of the thermocouple response curve changed slightly, from the expected curve for a gas flow with increasing droplet concentration. The potential exists for deriving a measure of the droplet density from the response curve shape and thus applying corrections to measurements of mean temperature to provide a more representative gas temperature.

High speed cine films have been taken of the sprays. The most striking features of these films were large eddies which could be followed, individually, downstream from approximately x = 20 mm to, at least, x = 150 mm. These eddies are considered to be 'coherent structures' and such structures have been shown to be important in most types of turbulent shear flow.[11, 12] The existence of coherent structures in both vaporising sprays and spray flames has very significant effects on flow and flame structure. In particular it can be seen that the smaller droplets remain within these eddies, whilst the larger droplets penetrate the eddy boundaries and can leave the region of rotational, turbulent gas flow. Thus physically realistic models should include effects of eddy structure in making calculations of the dispersion, environments and ballistics of droplets as a function of droplet size. This topic will be considered in the next stage of this research which concerns time-dependent

measurements of droplet-gas interactions, droplet size/velocity correlations and also comparisons with modelling predictions and assumptions.

## 6. CONCLUSIONS

(1) The laser tomography technique provides a rapid and accurate means for the detailed mapping of spray structure in terms of droplet sizes and concentration.

(2) The technique also enables measurement of spray vaporisation, provided that measurements of droplet velocities can be obtained.

(3) The computerised fine wire thermocouple response characteristics can be used to provide a convenient means for measuring gas velocity in both hot and cold sprays.

(4) Droplet impaction significantly influences thermocouple mean temperature measurements, even in dilute sprays. However the potential exists for correcting such measurements.

(5) In the particular twin-fluid spray studied here, a spatially segregated distribution of droplets was found near the atomiser, with a fairly dilute and monodisperse sheath of larger droplets surrounding a polydisperse dense core.

(6) With increasing distance downstream this segregation was reduced by the dispersion of droplets by the turbulence. A coherent, large eddy structure appeared to be the dominant mechanism of droplet dispersion.

(7) The tomography measurements demonstrated the preferential vaporisation of the smaller droplets.

## ACKNOWLEDGEMENT

The authors gratefully acknowledge support for this work by the NASA-Lewis Research Center under Grant No. NSG-7517.

## REFERENCES


1. Styles, A. C. and Chigier, N. A., "Combustion of air blast atomised spray flames", 16th Symposium (International) on Combustion, pp. 619-630, The Combustion Institute, Pittsburgh, 1977.

2. Founti, M. and Whitelaw, J. H., "Measurements and calculations of the kerosene-fueled flow in a model furnace." Paper AIAA-80-0074, AIAA 18th Aerospace Sciences Meeting, Pasadena, Ca, January 1980.

3. Owen, F. K., "Measurements in combustion systems", Laser Velocimetry and Particle Sizing (Thompson and Stevenson, eds.), pp. 123-135, Hemisphere Publishing Corp., Washington, DC, 1979.

4. Labowski, M. and Rosner, D. E., "Conditions for group combustion of droplets in fuel clouds." Symposium on Evaporation-Combustion of Fuel Droplets, Division of Petroleum Chemistry, Am. Ch. Soc., 1976.

5. Swithenbank, J., Béer, J. M., Taylor, D. S., Abbot, D., and McCreath, C. G., "A laser diagnostic technique for the measurement of droplet and particle size distribution", Experimental Diagnostics in Gas-Phase Combustion Systems, Progress in Astronautics and Aeronautics 53, pp. 421-447, (B. T. Zinn, ed.), 1977.

6. Felton, P. G., "Measurement of particle/droplet size distributions by a laser diffraction technique." 2nd European Symposium on Particle Characterization, PARTEC, Nürnberg, pp. 662-680, September 1979.

7. Yule, A. J., Ah Seng, C., Felton, P. G., Ungut, A., and Chigier, N. A., "A laser tomographic investigation of liquid fuel sprays", 18th Symposium (International) on Combustion, Waterloo, Canada, August 1980.

8. Yule, A. J., Cox, N. W., and Chigier, N. A., "Measurement of particle size in sprays by the automated analysis of spark photographs", Particle Size Analysis (Groves, ed.), pp. 61-73, Heyden, London, 1978.

9. Yule, A. J., Taylor, D. S., and Chigier, N. A., "Thermocouple signal processing and on-line digital compensation", AIAA J. En. 2, pp. 223-231, 1978.

10. Ungut, A., Yule, A. J., Taylor, D. S., and Chigier, N. A., "Particle size measurement by laser anemometry", AIAA J. En. 2, pp. 330-336, 1978.

11. Davies, P. O. A. L., and Yule, A. J., "Coherent structures in turbulence", J. Fluid Mech. 69, p. 513, 1975.

12. Yule, A. J., "Investigations of eddy coherence in jet flows." Proceedings of International Conference on Role of Coherent Structures in Modelling Turbulence and Mixing, Madrid, 25-27 June, 1980, Springer Verlag, 1980.

TABLE 1

INITIAL CONDITIONS AT ATOMISER (SEE ALSO FIG. 2)

| | | |
|---|---|---|
| Volume flow rate of kerosene | = | $9 \times 10^{-2}$ ml/s |
| Volume flow rate of atomising air (STP) | = | $1.52 \times 10^{2}$ ml/s |
| Average velocity of kerosene at atomiser nozzle | = | 0.46 m/s |
| Average velocity of atomising air at atomiser nozzle | = | 105 m/s |
| Secondary air velocity | = | 5 m/s |
| Mass flow rate of kerosene ($m_F$) | = | 0.072 g/s |
| Mass flow rate of atomising air ($m_A$) | = | 0.187 g/s |
| Initial momentum of atomising air ($M_A$) | = | $1.96 \times 10^{-2}$ Kgm/s$^2$ |
| Initial momentum of kerosene ($M_F$) | = | $3.31 \times 10^{-5}$ Kgm/s$^2$ |
| Atomiser air/fuel mass ratio ($m_A/m_F$) | = | 2.6 |
| Atomiser fuel/air volume flow ratio | = | $5.92 \times 10^{-4}$ |
| Reynolds number for kerosene flow at atomiser | = | $10^3$ |
| Reynolds number for atomising air | = | $2.9 \times 10^3$ |

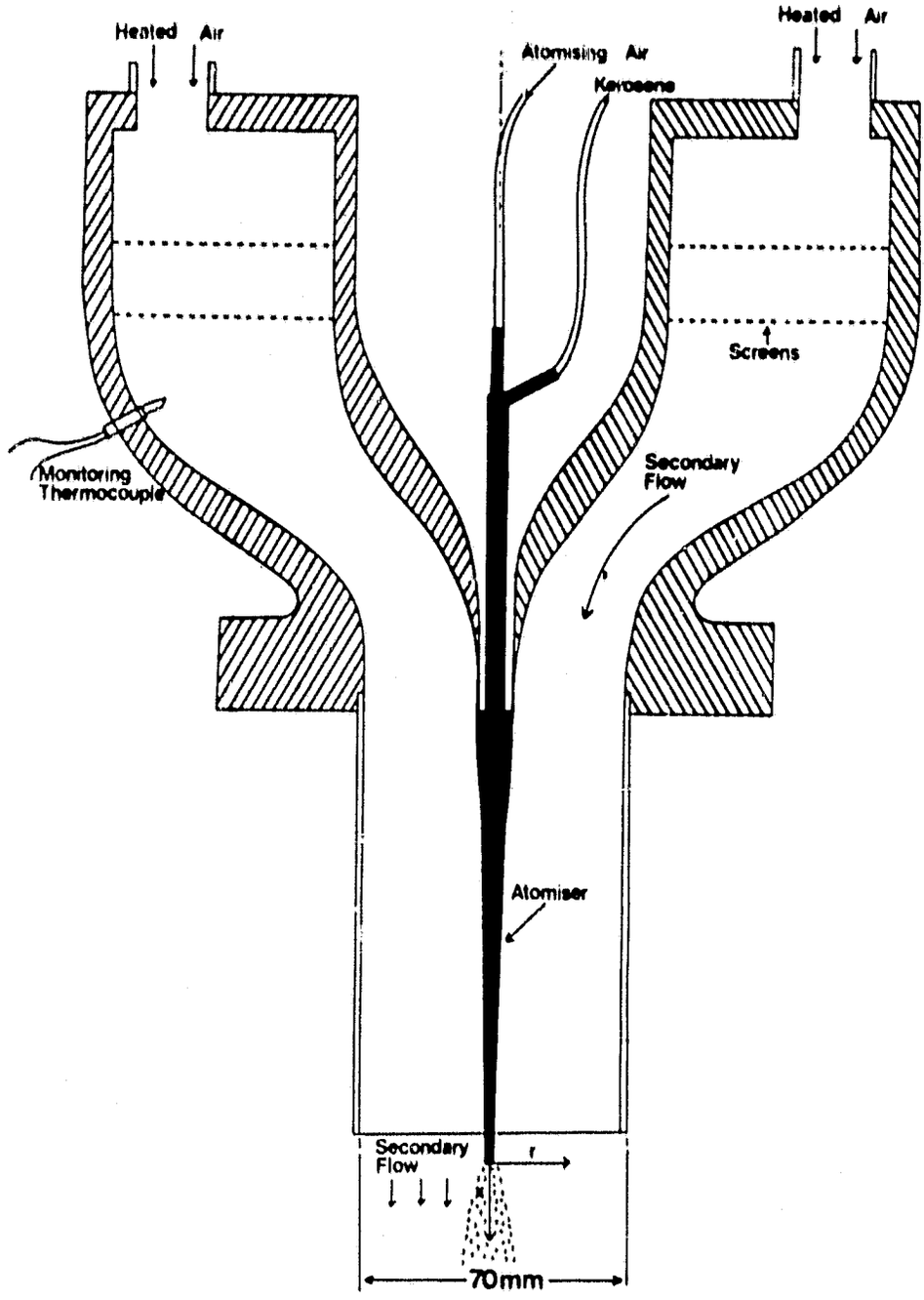


FIG. 1. Apparatus for the investigation of fuel spray in a heated secondary air flow.

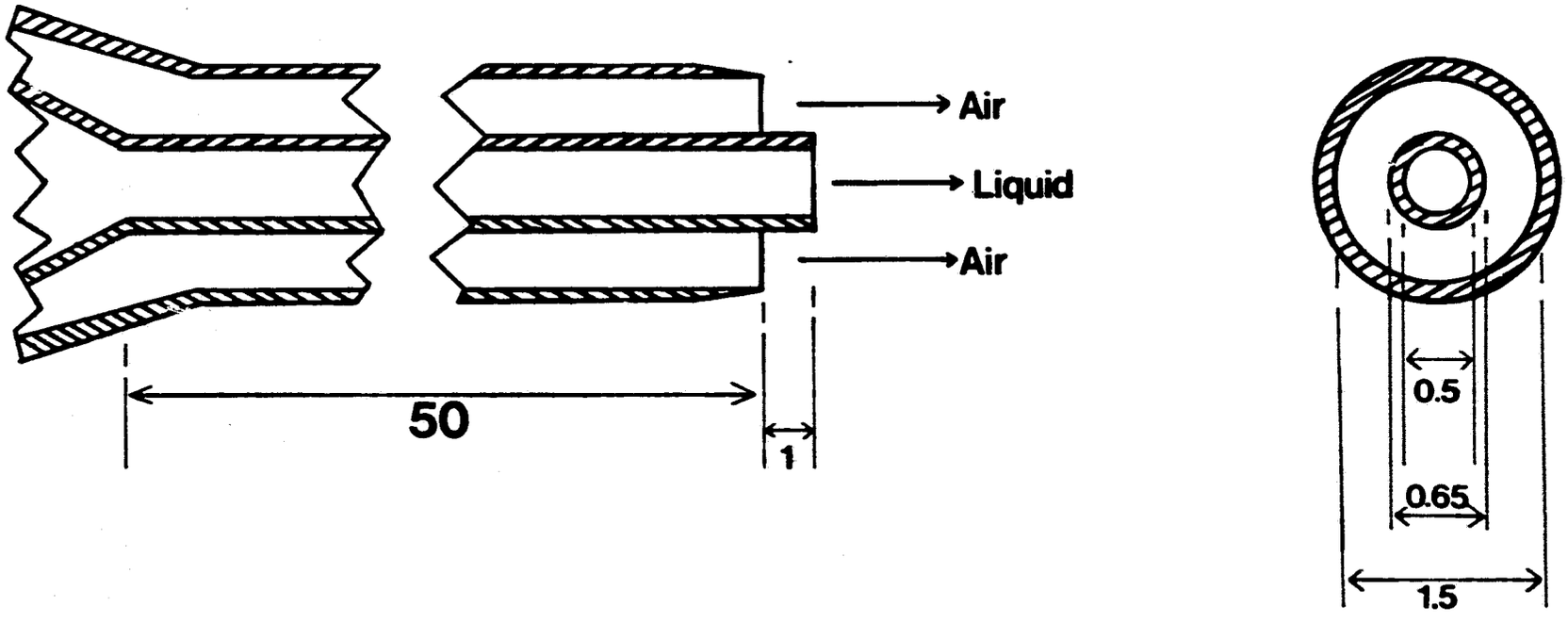


FIG. 2. Design of atomiser tip.

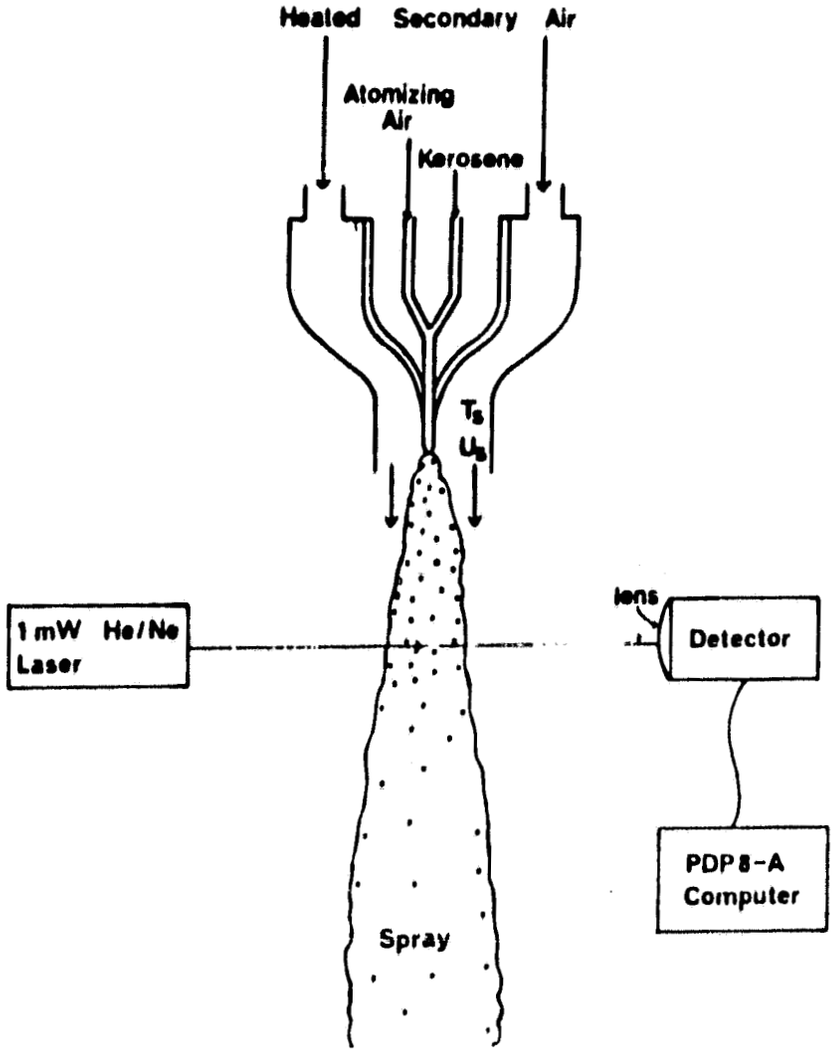


FIG. 3. Light scattering investigation of a fuel spray.

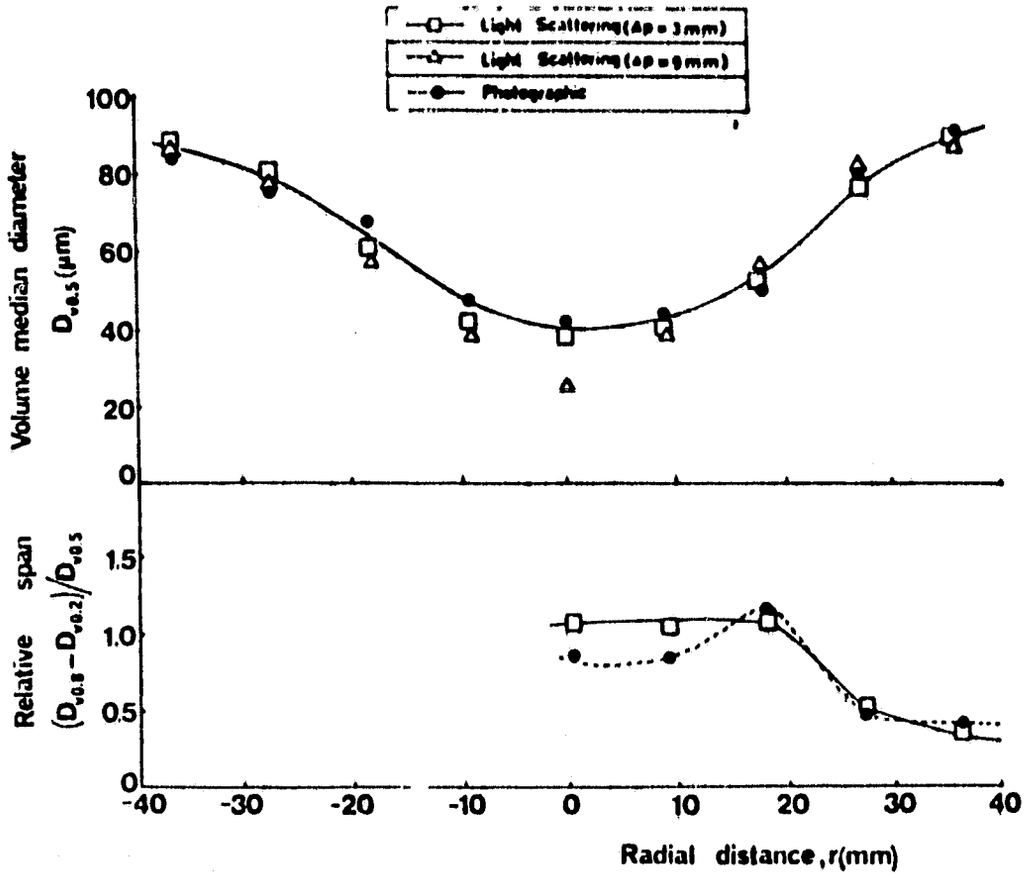


FIG. 4. Comparison of laser tomographic and photographic measurements of mass mean diameters in a water spray (ref. 7) where $\Delta p$ is the separation between laser scans.

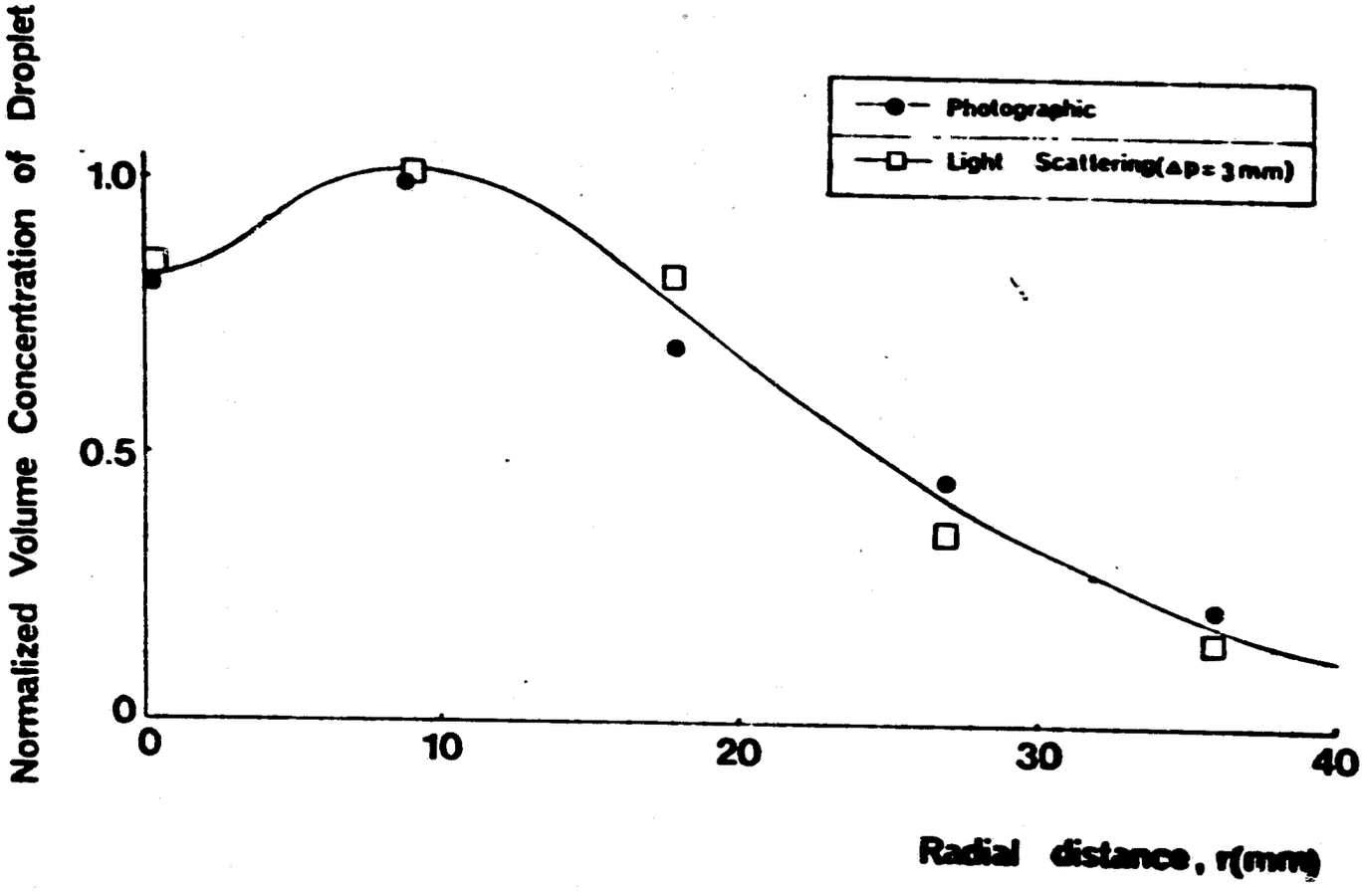


FIG. 5. Comparison of laser tomographic and photographic measurements of droplet volume concentrations in a water spray (ref. 7).

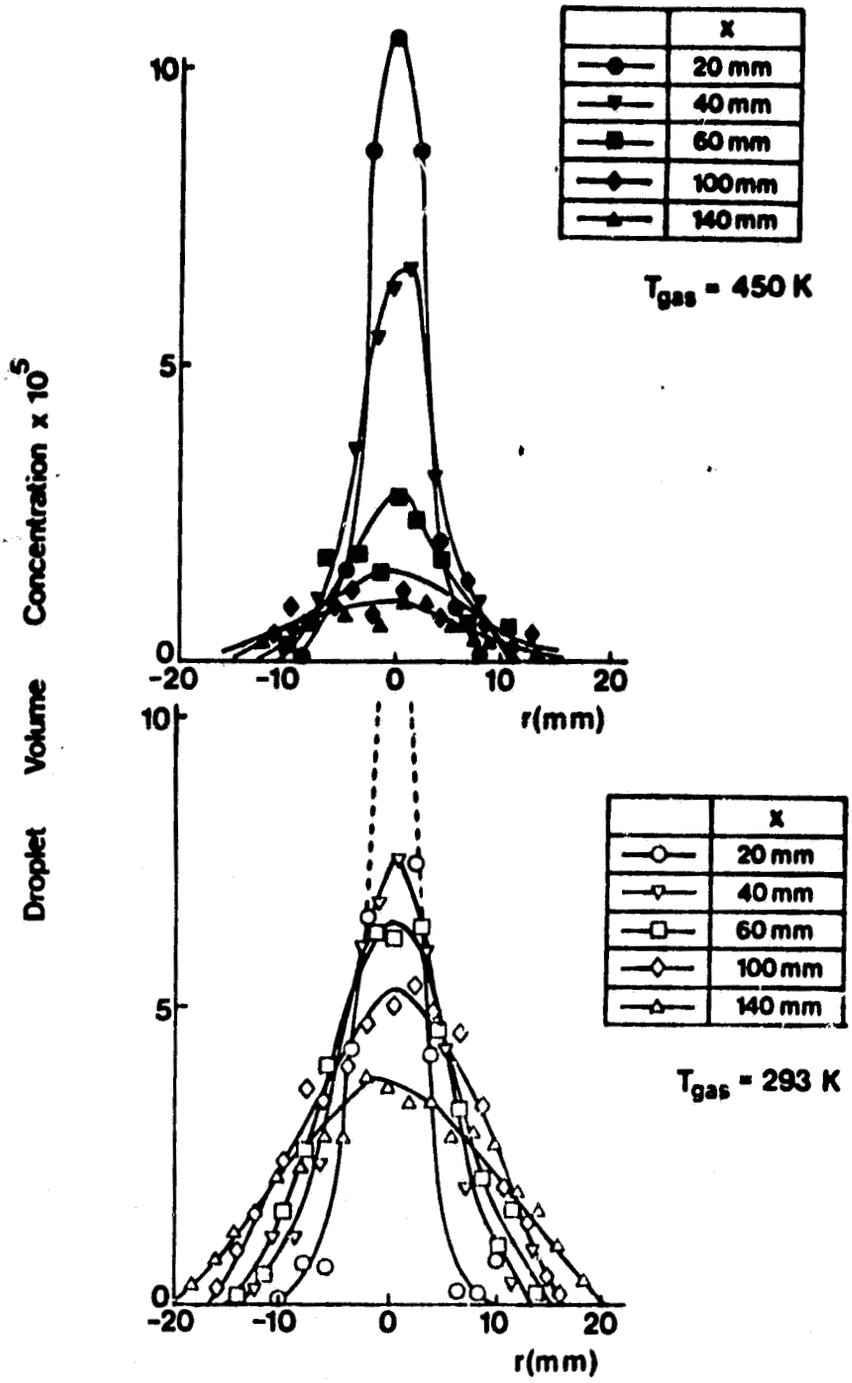


FIG. 6. Droplet volume concentrations in cold and hot kerosene sprays measured by laser tomography (caser (ii) and (iv)).

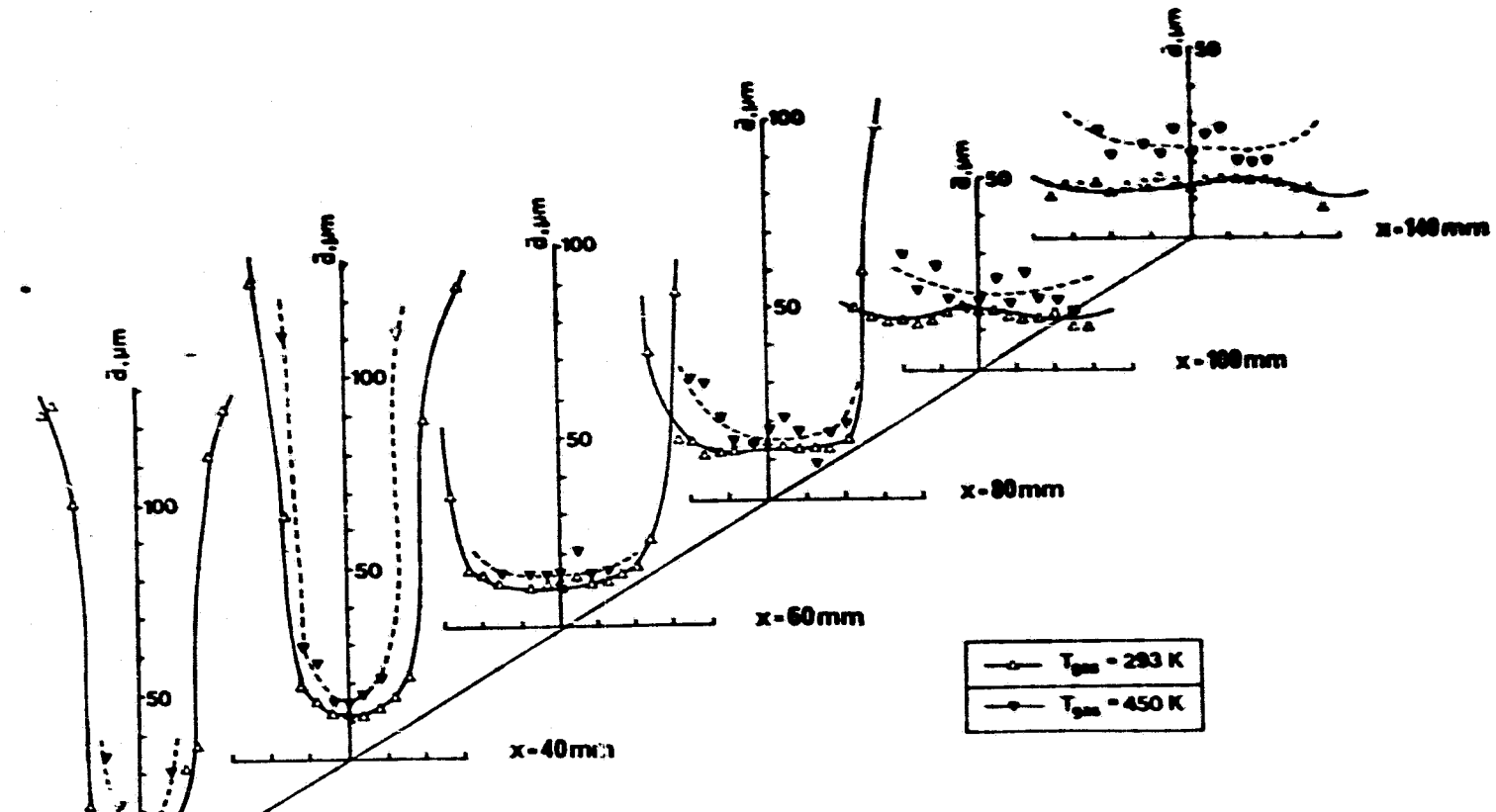


FIG. 7. Distributions of mass mean droplet diameter in cold and hot sprays measured by laser tomography.

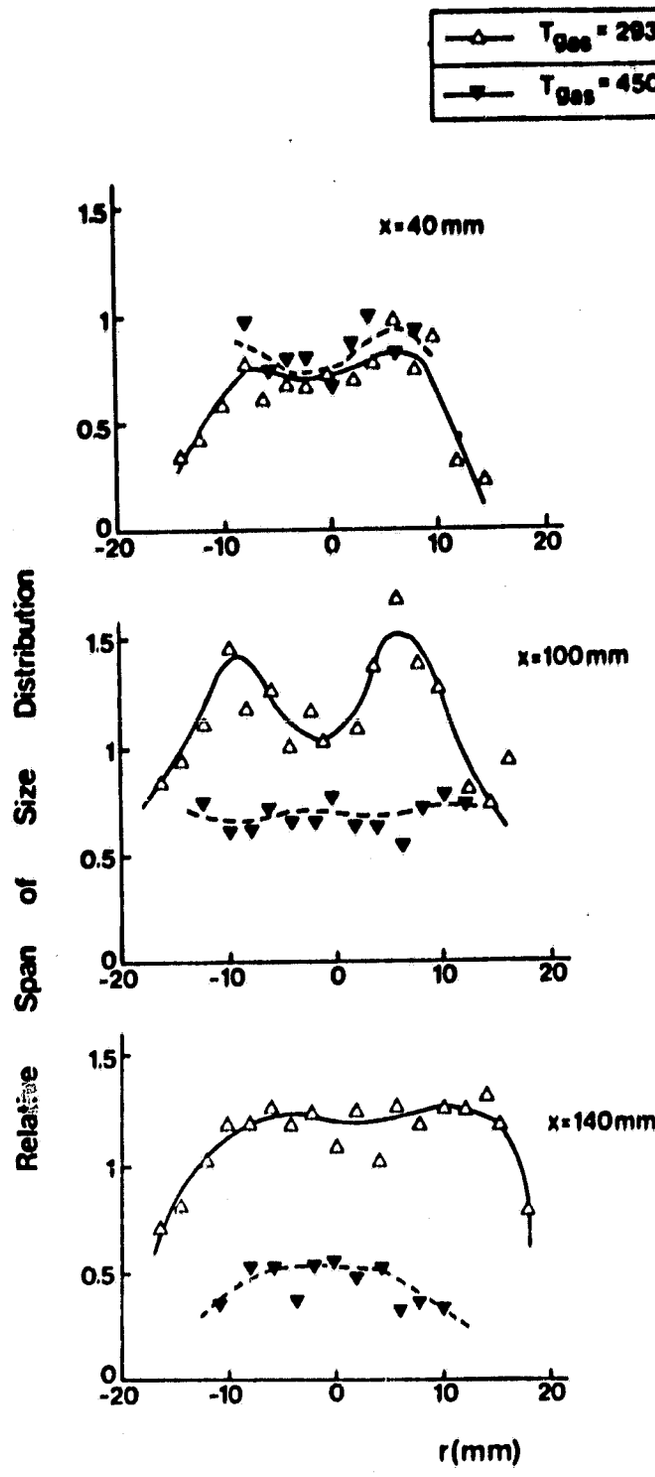


FIG. 8. Distributions of span of droplet size distributions in cold and hot sprays measured by laser tomography.

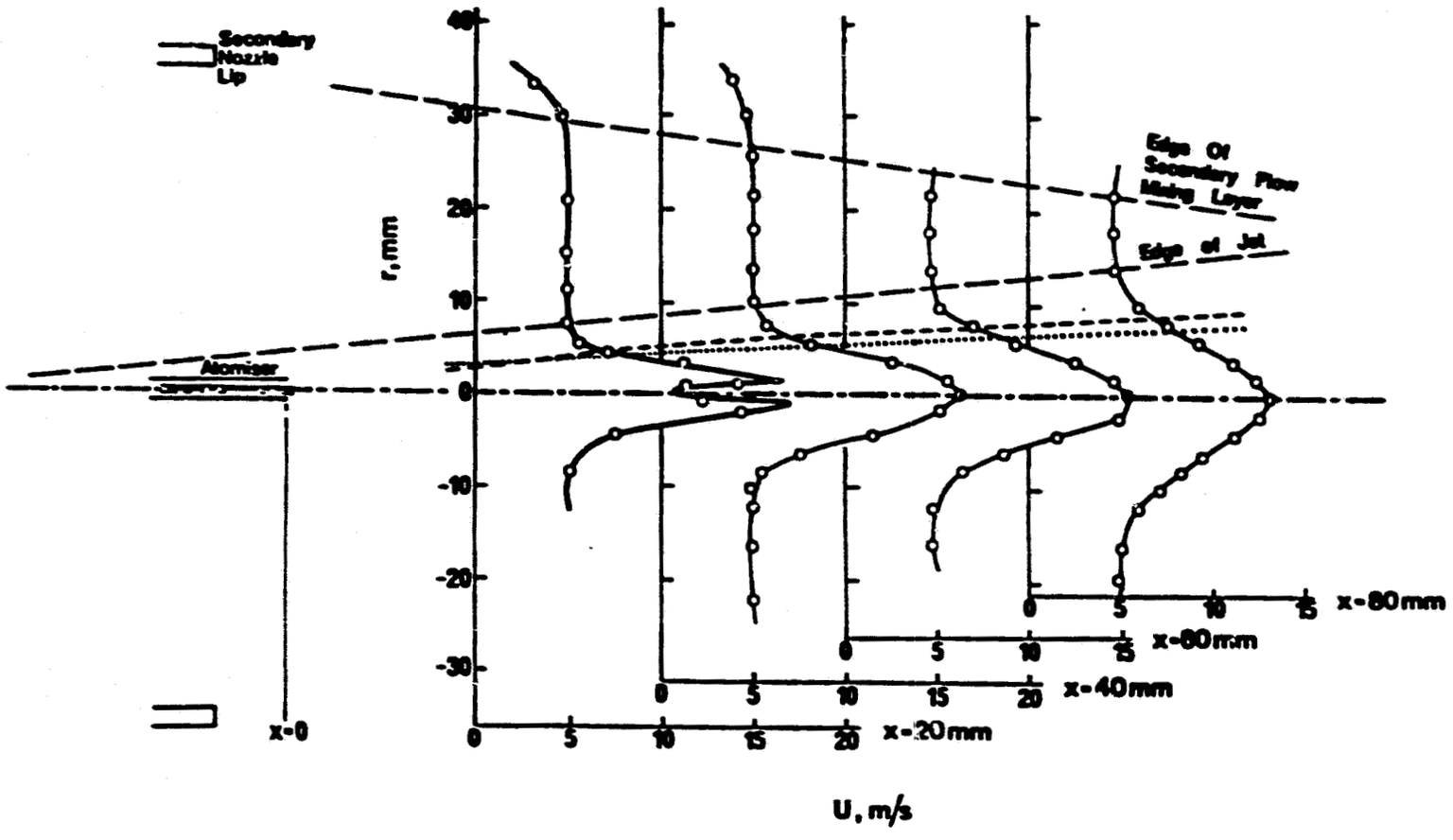


FIG. 9. Laser anemometer mean velocity measurements in cold flow. Half widths:---- droplet concentration,..... velocity.

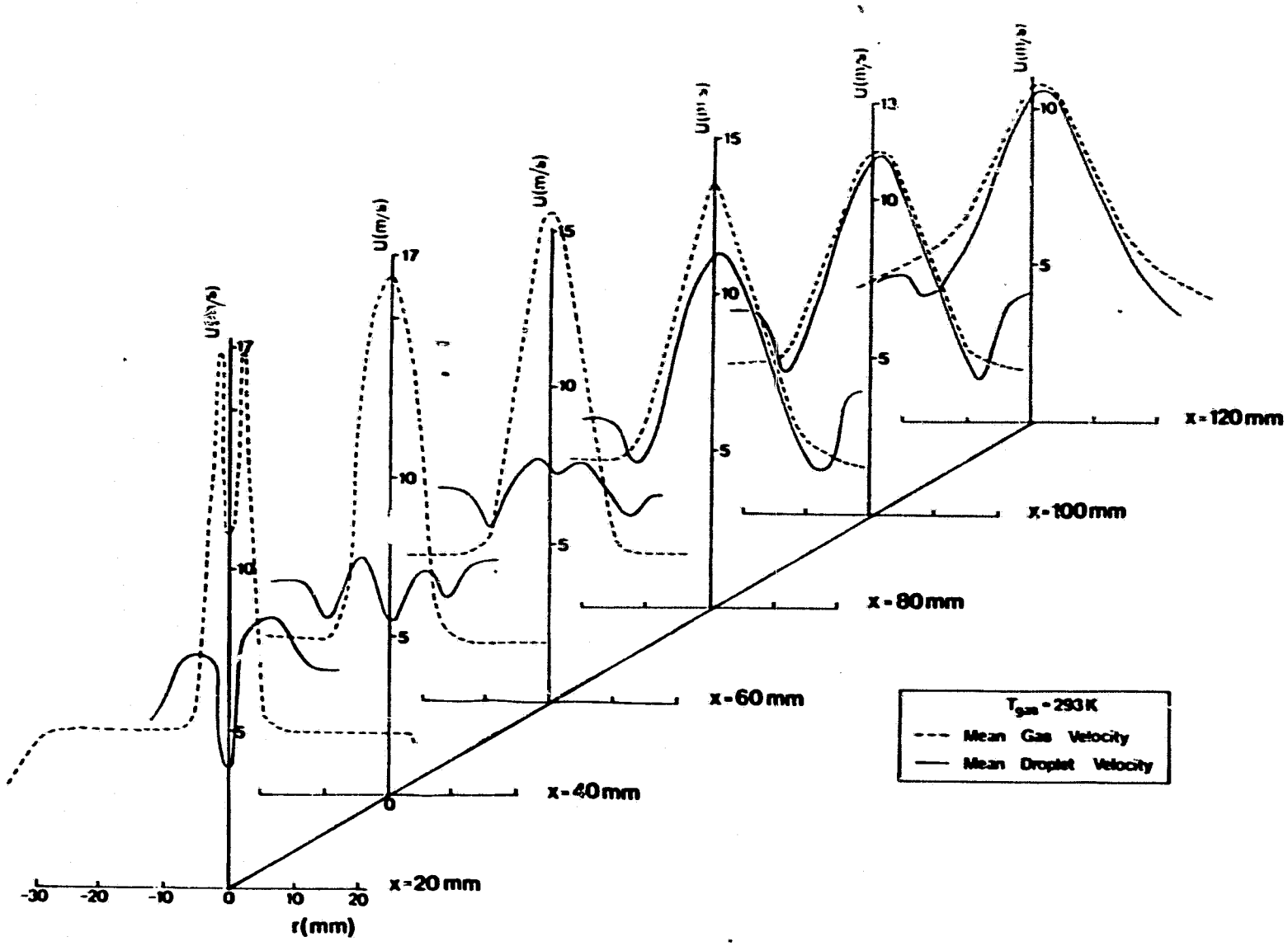


FIG. 10. Comparison of laser anemometer measurements of mean gas velocity (without droplets) and mean droplet velocity in cold flow (cases (i) and (ii)).

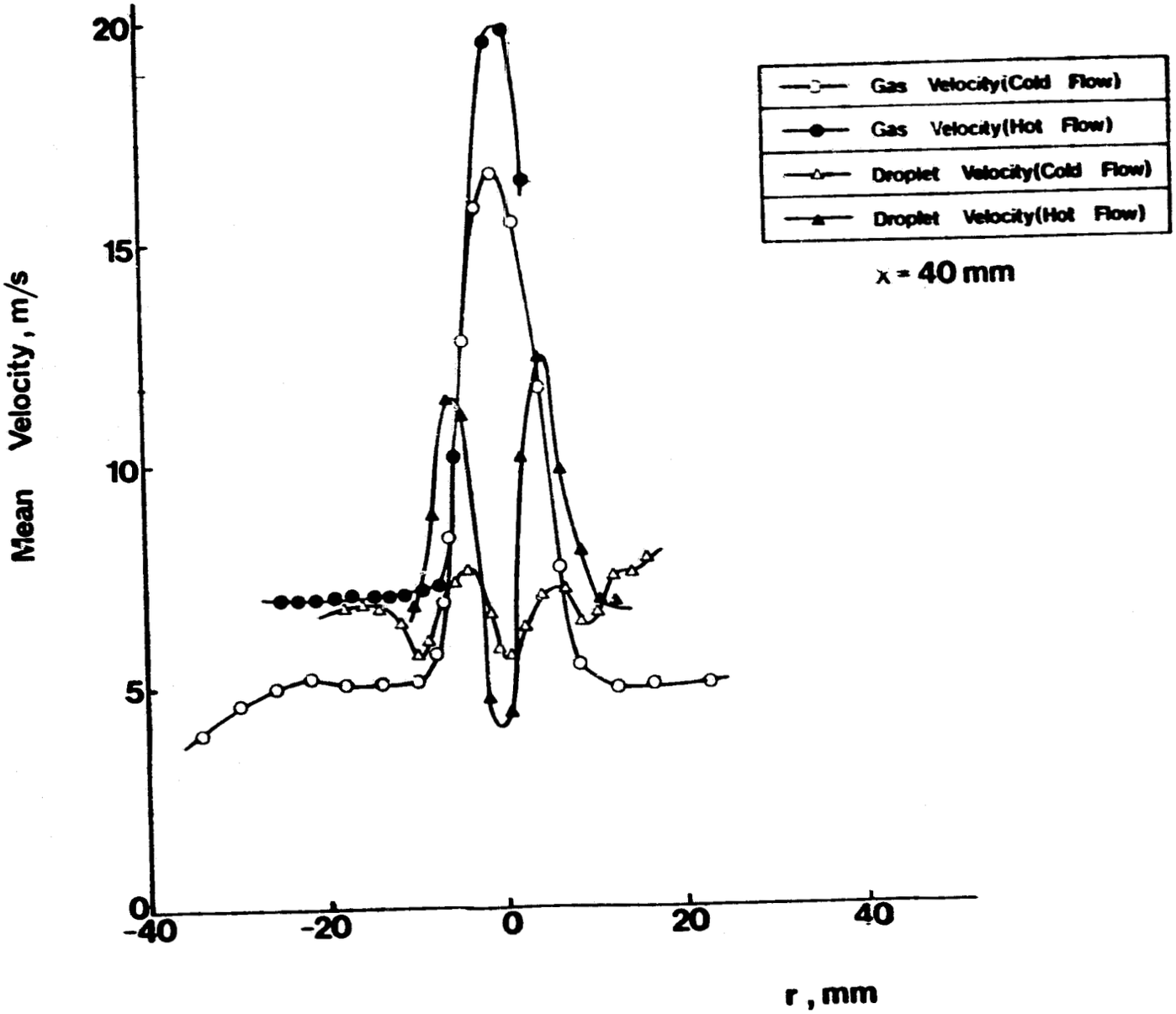


FIG. 11. Gas and droplet velocities in 'hot' and 'cold' flows at x = 40 mm. (All LDA measurements except for hot gas velocity, which is measured using a thermocouple.)

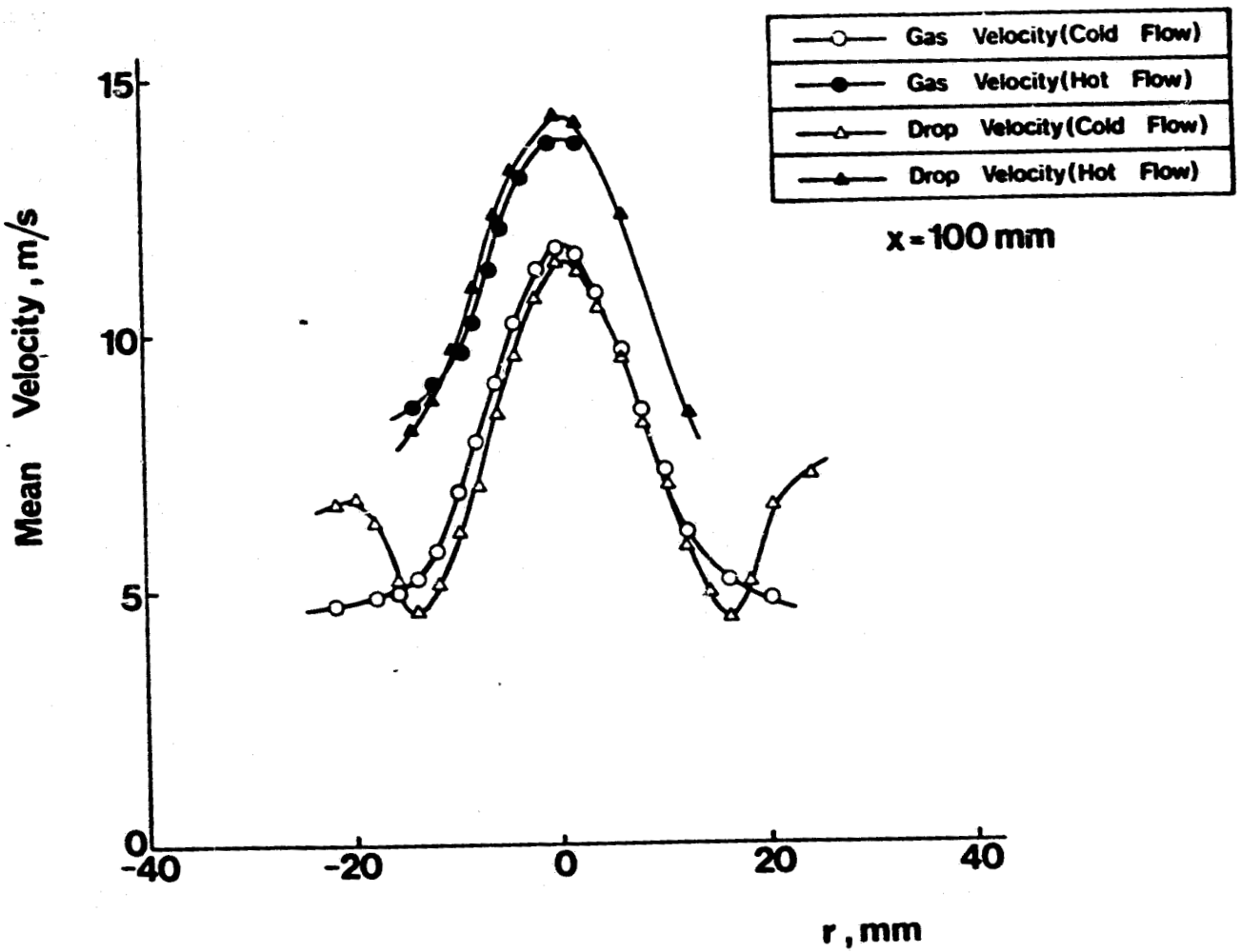


FIG. 12. Gas and droplet velocities in 'hot' and 'cold' flows at x = 100 mm.

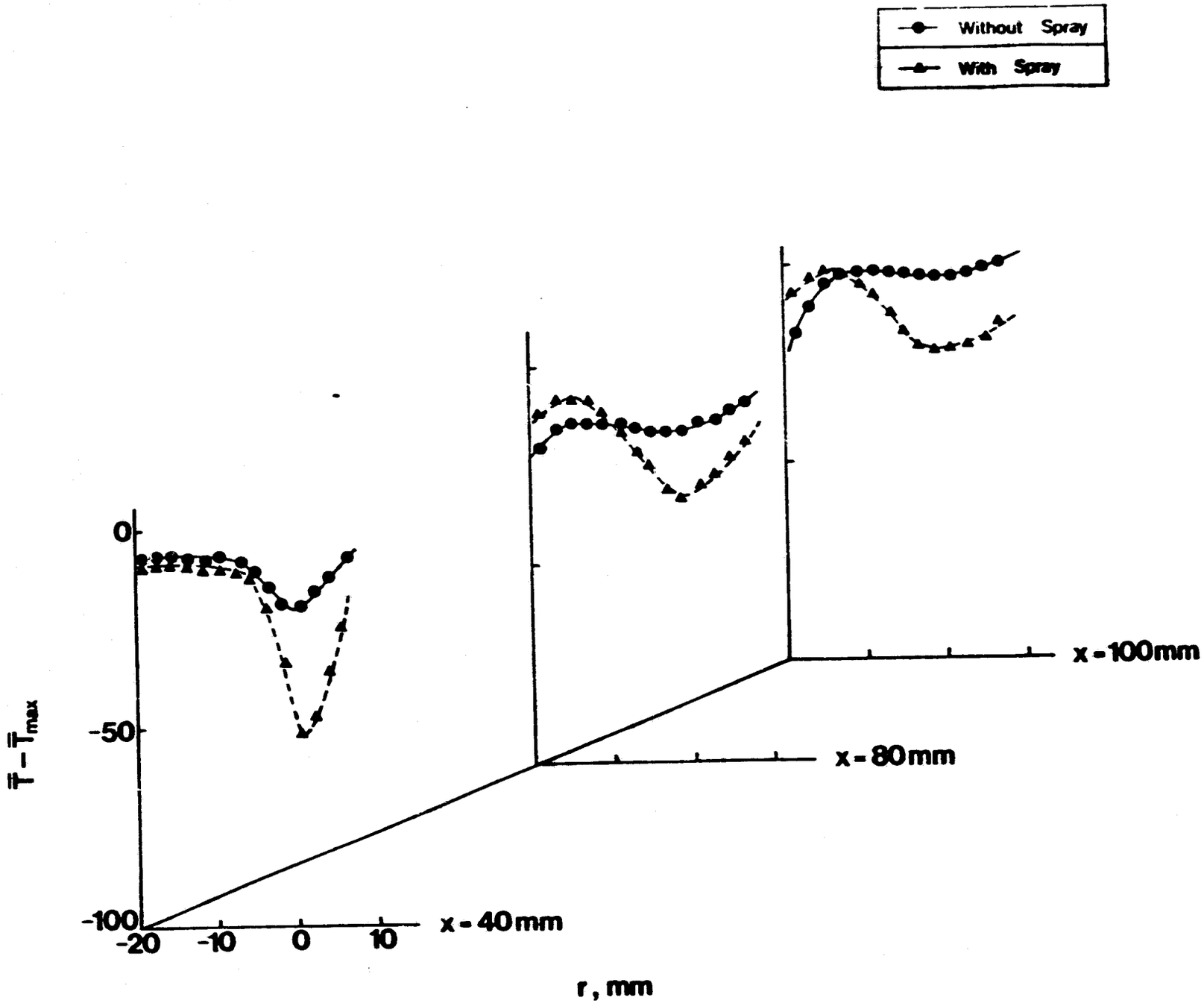


FIG. 13. Mean temperatures measured in hot flow, with atomising air, with and without droplets (cases (iii) and (iv)).

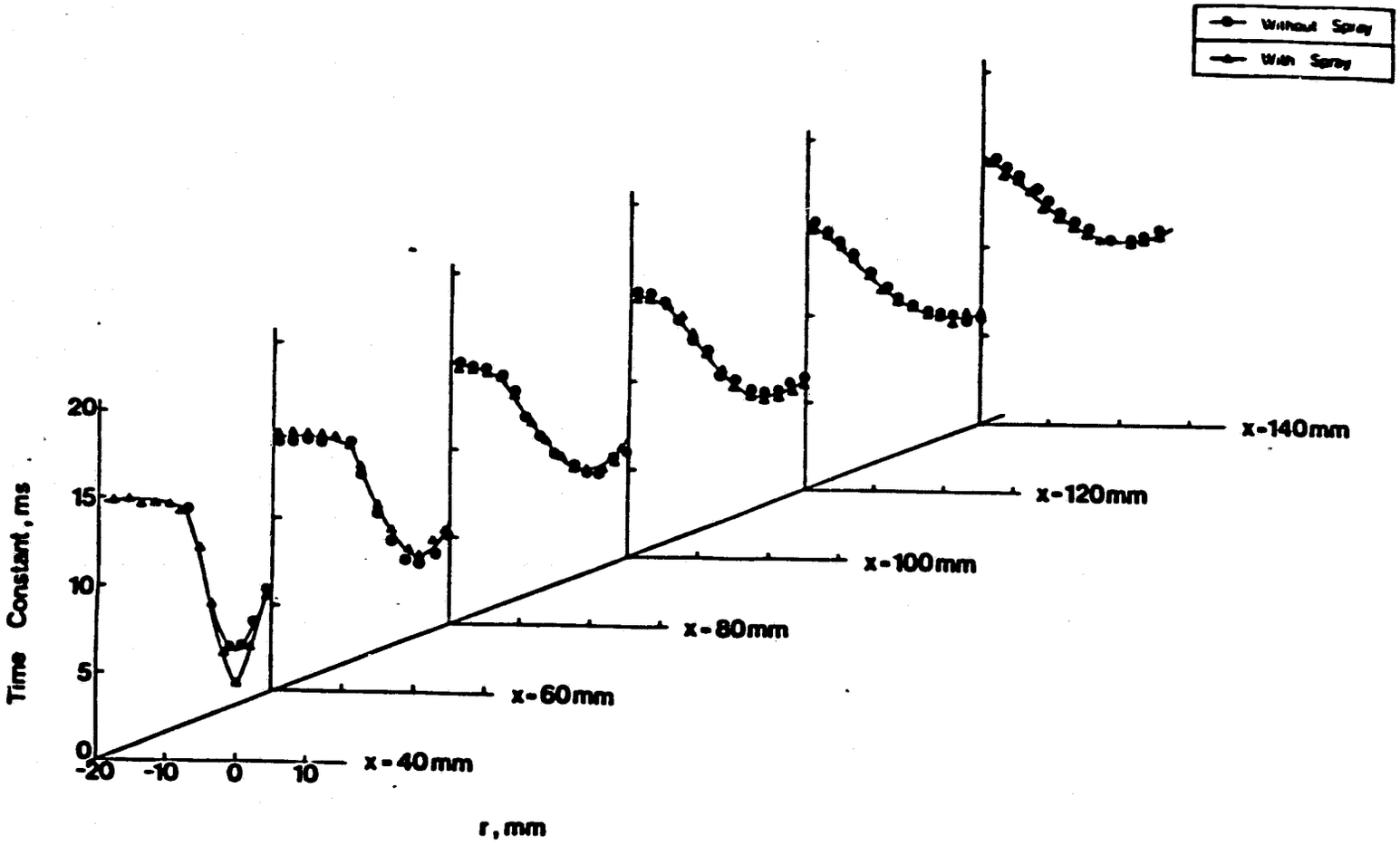


FIG. 14. Thermocouple time constant measured in hot flow, with and without droplets.

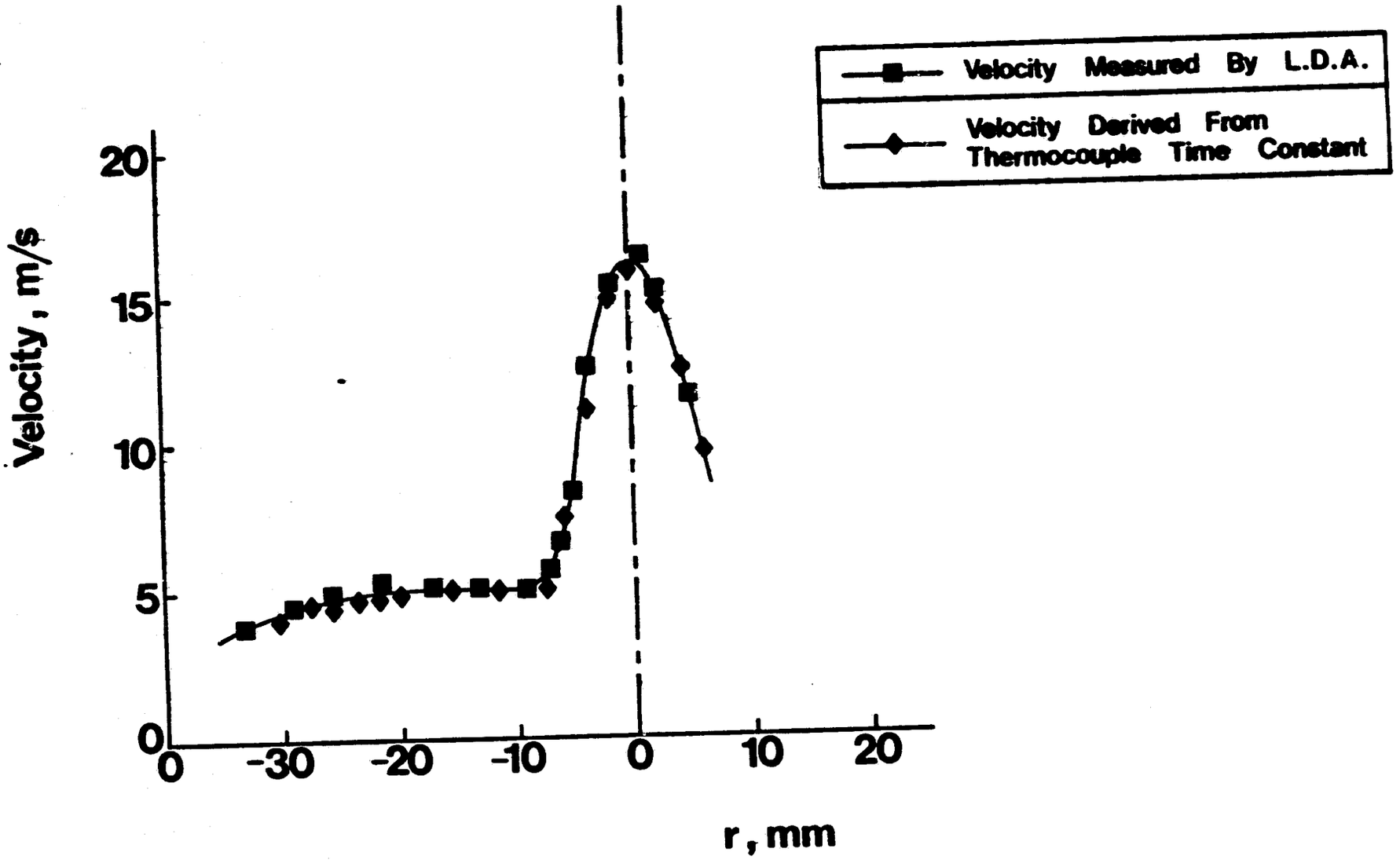


FIG. 15. Comparison of mean velocity measurements by thermocouple time constant and laser anemometer, for cold flow without droplets.

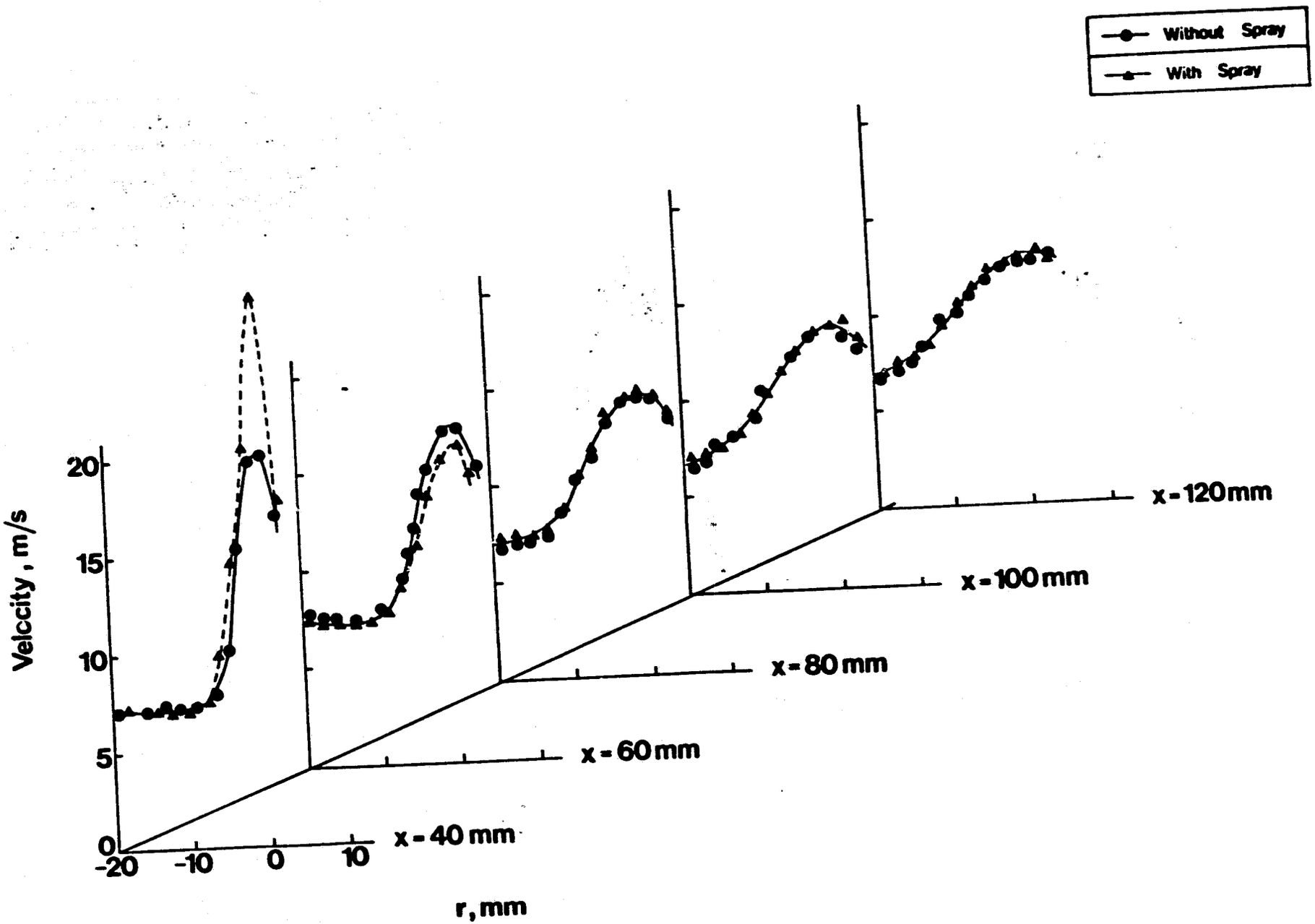


FIG. 16. Comparison of mean velocities derived from thermocouple time constant in hot flow, with and without droplets.

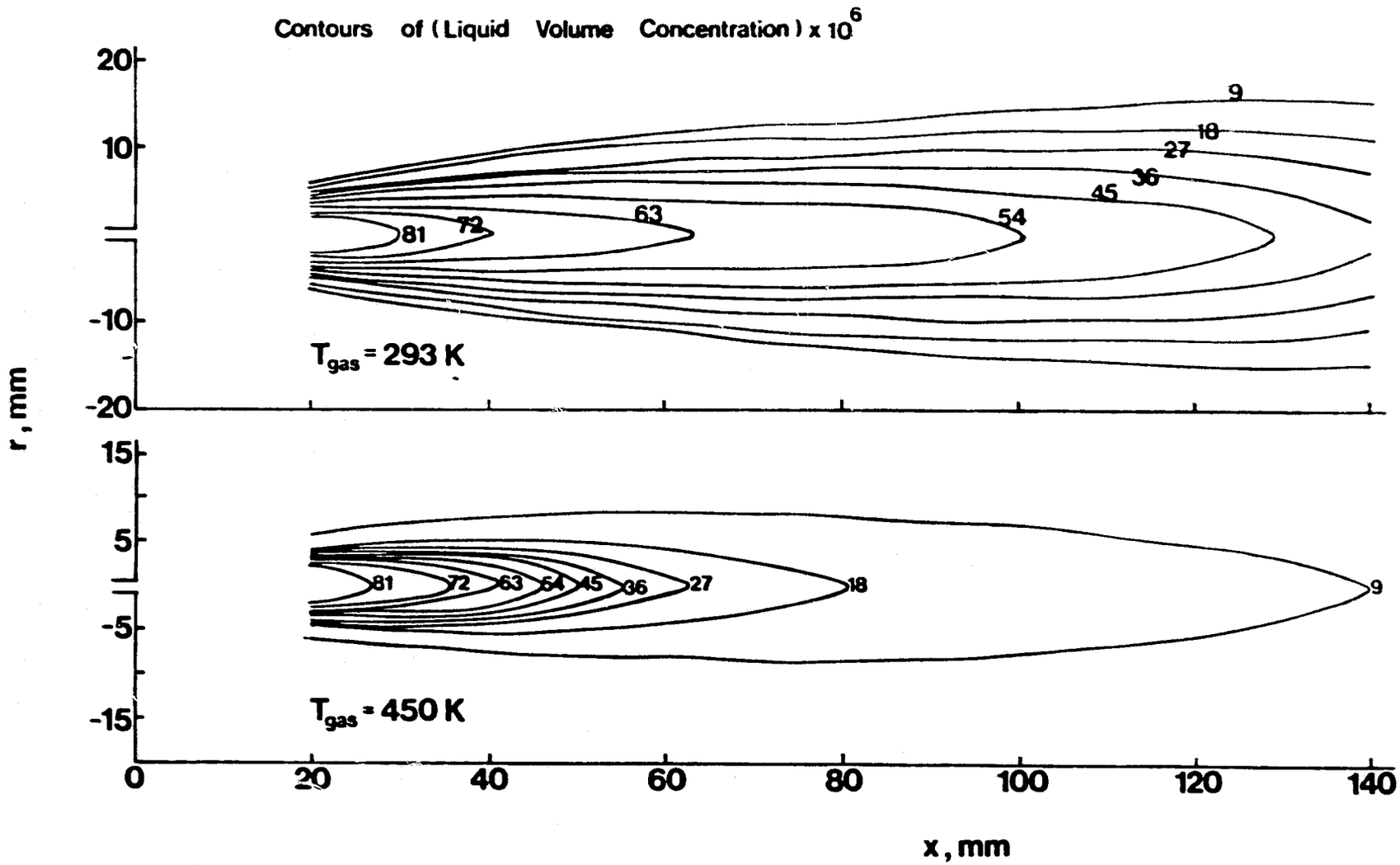


FIG. 17. Iso-concentrations (by volume) of liquid phase in sprays in cold and hot secondary flows.

FIG. 18. Shadow photograph of cold spray near atomiser (magnification 16.5).

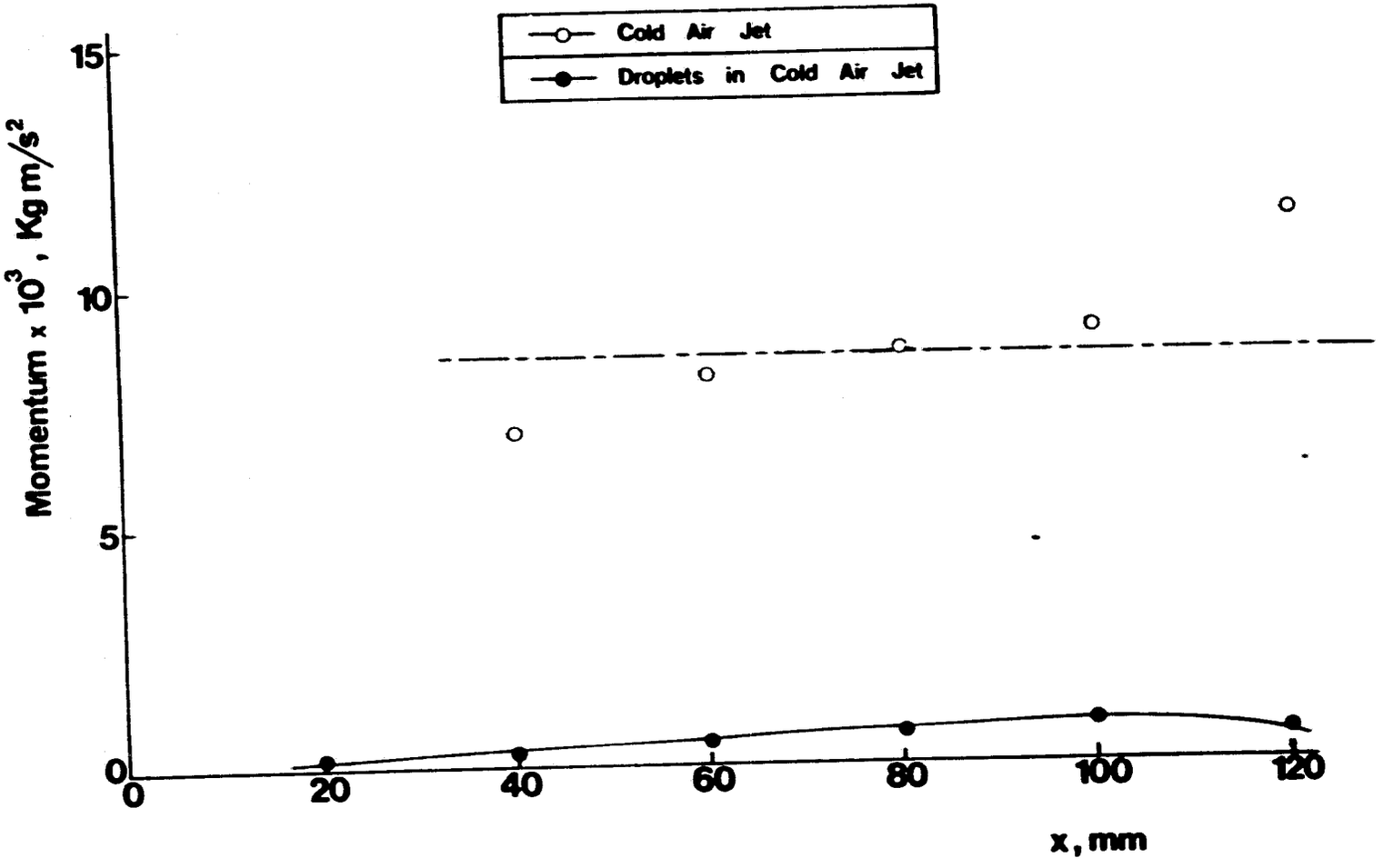


FIG. 19. Momenta of gas and liquid phases in cold spray (by integration of velocity and concentration data).